

Invited Paper

Terahertz imaging for security – algorithm and system realization

Chao Li ^{1,2*}, and GuangYou Fang ^{1,2}¹ The Key Laboratory of Electromagnetic Radiation and Sensing Technology, Chinese Academy of Sciences, BeiJing, China² Institute of Electronics, Chinese Academy of Sciences, BeiJing, China*² Email: cli@mail.ie.ac.cn

(Received August 18, 2015)

Abstract: Terahertz (THz) wave has unique properties due to its special position in the electromagnetic spectrum, which lies in the gap between the electronics and photonics. In recent years, imaging and sensing with EM radiation in Terahertz band has aroused considerable interests and is found to be promising for plenty of applications, such as security and safety screening, process monitoring and non-destructive materials testing. Besides being limited by the maturity of electronic components, design and realization of imaging systems at THz band with high performance is a complex issue which is dependent on variety of key parameters such as spatial resolution, sensitivity, target contrast, target identification, and so on. This paper describes and summarizes some background on THz imaging, and the recent progress on the research of THz imaging and sensing at Institute of Electronics, Chinese Academy of Sciences, both in theoretical and some system engineering aspects. The imaging scheme and reconstruction algorithm with synthesized aperture concept was extended to THz band. The relationships between the image qualities and the parameters of quasi-optical transceivers were quantitatively evaluated for the guidance of system development. Some novel THz imaging concepts based on sparse information were also introduced, such as the single frequency adaptive focusing with minimum-entropy (ME) method, and THz surface layer reconstruction with sparse random step frequency. Based on the combination of the synthesized aperture concept, the novel beam scanning method, and THz frequency modulated continuous wave (FMCW) transceiver, three-dimensional (3D) imaging radar in sub-THz band with real-time capability was developed, which has potential applications for security screen.

Keywords: Terahertz imaging, Security, Reconstruction algorithm, Synthesized aperture technique, Beam scanning

doi: [10.11906/TST.19-36.2016.03.03](https://doi.org/10.11906/TST.19-36.2016.03.03)

1. Introduction

Terahertz (THz) wave has unique properties due to its special position in the electromagnetic (EM) spectrum, which lies in the gap between the electronics and photonics. Generally, THz waves are referred to the spectrum from 0.1 and 10 THz (or more strictly with lower bound limited to be 0.3 THz). Its lower bound overlapped with the submillimeter wave and its upper bound overlapped with the infrared. So both the technologies borrowed from the electronics and the photonics play important roles in this band [1-4]. Unlike optical and infrared radiation, THz

waves offer the property of being able to ‘see through’ obscuring materials such as clothing, cardboard, plastics, and wood with relatively little loss. Compared to microwave and lower radio frequency wave, THz wave has shorter wavelength which results in better spatial resolution and makes the objects easier to identify. Additionally, the vibrational spectral characteristics of biomolecules usually lie in the range with wave numbers between 3.3 and 333 cm^{-1} [5]. Hence, complementary information to traditional spectroscopic measurements on low-frequency bond vibrations, hydrogen bond stretching, and bond torsions in liquids and gases can be obtained in THz band. The above unique advantages make THz imaging and sensing promising for plenty of applications, such as personal screening for airport or corporate security [6-10], surrounding surveillance for safety [11], non-contact and non-destructive materials testing [12-13], biomedical analysis and diagnostics [14-16], and so on.

2. Some background on terahertz imaging for security

2.1 The atmospheric effects

For long distance applications, the atmospheric attenuation is always an important aspect that has to be considered. The atmospheric attenuation below 1 THz is shown in Fig.1 for different atmospheric conditions, from low atmospheric attenuation in the winter, to the extremely high levels in tropical climates [17]. The attenuation rises with frequency due to the rotational absorption lines of molecular oxygen and water vapor. The transmission windows at the lower band in terahertz region are commonly interested by the researchers and the engineers.

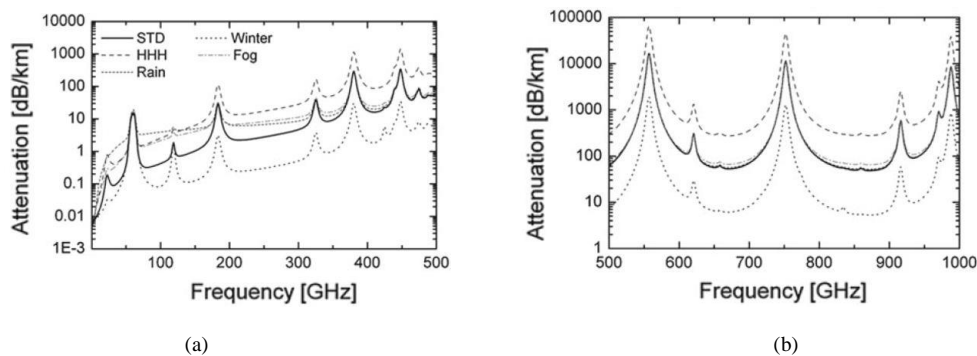


Fig. 1 Atmospheric attenuation in the band up to 1 THz for various weather conditions [17]: STD—Standard US atmosphere; HHH—Hot and humid; Winter— 10 C ; Fog— 100 m visibility, Rain— 4 mm/hr

2.2 The compromise between ‘see through’ and ‘target identification’

In imaging for personal security, the threats concealed on body are expected to be identified with high probability and low false alarm rate. Generally, the imaging scheme can be divided into two types, the passive and the active imaging. For passive imaging, the receivers record the natural radiation emitted and reflected by the object and the surroundings. While for active

imaging, only the coherent reflection reflected by the object from the illumination of the transmitter is interested, and all the information useful in the passive imaging becomes the noise in its active counterpart.

Regardless of active or passive scheme, the contrasts of the optical properties for different materials are always important for the target identification. In passive system, the emissivity is concerned while in the active system, reflectivity is the important parameter. From Table I [6], we can find that, compared to explosives, metal has more contrast to the human skin and is much easier to be detected in MMW and THz band. Especially as the frequency goes up from 100 GHz to 1 THz, the emissivity and the reflectivity of the human being skin become more and more distinct from that of the metal, which results in a higher possibility for metal detection from human body. Another aspect has to be concerned is the transmission property of the cloth. It's seen from Fig.2 that, when the frequency goes from 100 GHz to 1 THz, the cloth becomes more and more opaque [18-21]. Fortunately, most of the cloth, such as denim, sweatshirt, and T-shirt is still well transparent to the waves below 500 GHz. So, no matter whether using high frequency or low frequency, one must make a compromise to choose for special applications.

Tab. I Optical Properties of 5mm thick explosives, skin, metal, denim and T-shirt [6]

	Emissivity (ϵ)			Reflectivity (r)			Transmission (t)		
	100 GHz	500 GHz	1 THz	100 GHz	500 GHz	1 THz	100 GHz	500 GHz	1 THz
Explosive on skin	0.76	0.95	0.94	0.24	0.05	0.06	0	0	0
Metal	0	0	0	1	1	1	0	0	0
Skin	0.65	0.91	0.93	0.35	0.09	0.07	0	0	0
Denim	0.09	0.49	0.85	0.01	0.01	0.05	0.9	0.5	0.1
tee-shirt	0.04	0.2	0.3	0	0	0.05	0.96	0.8	0.65

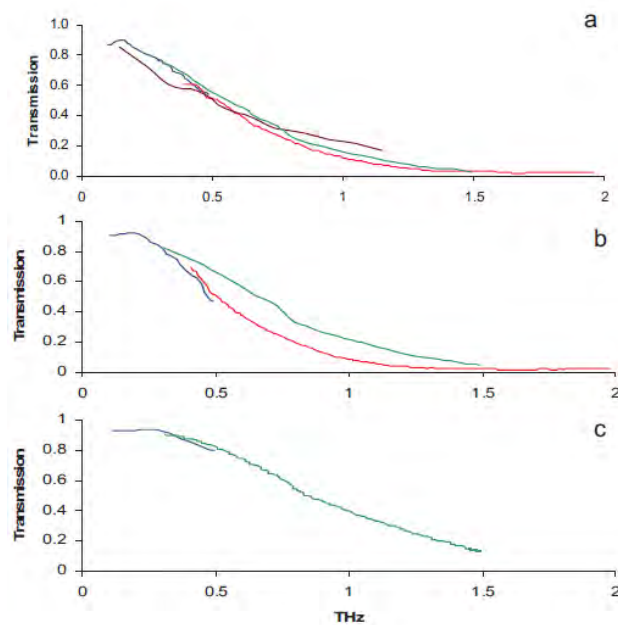


Fig. 2 Transmission of (a) Denim, (b) Sweatshirt and (c) Tee-shirt (red Gatesman et al. [18], green Dichinson et al. [19], brown Bjjarnson et al.[20], blue Appleby et al. [21])

2.3 Safety level of maximum permissible exposure (MPE)

For active imaging, another aspect which has to be concerned is the safety level of maximum permissible exposure (MPE) for human's body. So far, the MPE below 300 GHz can be referred in IEEE standard [22]. For 300 GHz, the maximum value is 10 Watts per square meter. For near distance imaging, a dynamic range of 40 dB or more can be achieved under the illumination of 100 mW/m^2 , for both real aperture and synthesized aperture imaging upon the modern solid state source and coherent receiving technology in sub-THz band. Hence, to obtain active image with good quality with exposure far below the maximum permission is possible.

Tab. II IEEE Standard for Safety Levels of Maximum Permissible Exposure (MPE) for Human's body from 100 kHz-300 GHz [22]

Frequency range (MHz)	RMS electric field strength (E) ^a (V/m)	RMS magnetic field strength (H) ^a (A/m)	RMS power density (S) E-field, H-field (W/m ²)	Averaging time E ² , H ² or S (min)
0.1-1.0	1842	$16.3/f_M$	$(9000, 100\ 000/f_M^2)^b$	6
1.0-30	$1842/f_M$	$16.3/f_M$	$(9000/f_M^2, 100\ 000/f_M^2)$	6
30-100	61.4	$16.3/f_M$	$(10, 100\ 000/f_M^2)$	6
100-300	61.4	0.163	10	6
300-3000	-	-	$f_M/30$	6
3000-30 000	-	-	100	$19.63/f_G^{1.079}$
30 000-300 000	-	-	100	$2.524/f_G^{0.476}$
NOTE— f_M is the frequency in MHz, f_G is the frequency in GHz.				
^a For exposures that are uniform over the dimensions of the body, such as certain far-field plane-wave exposures, the exposure field strengths and power densities are compared with the MPEs in the Table. For non-uniform exposures, the mean values of the exposure fields, as obtained by spatially averaging the squares of the field strengths or averaging the power densities over an area equivalent to the vertical cross section of the human body (projected area), or a smaller area depending on the frequency (see NOTES to Table 8 and Table 9 below), are compared with the MPEs in the Table.				
^b These plane-wave equivalent power density values are commonly used as a convenient comparison with MPEs at higher frequencies and are displayed on some instruments in use.				

2.4 Progress in THz imaging for Security

In recent years, researchers have made rapid progress in THz imaging technologies and systems for potential security applications. The stand-off systems T5000 [23, 24] from Thruvision is a typical passive camera working at 0.25 THz band, utilizing multi-channel heterodyne down-conversion receivers to obtain high frame rate and coupled with reflective telescopic optics to achieve beam focusing. Cryogenically cooled bolometer arrays with high sensitivity (NEP~10-16 W/√Hz) have also been employed to develop passive camera prototypes, such as the SAFE-VISITOR system [25, 26] working at 0.35 THz band. For active security imaging, the promising candidates are the 0.35 THz and 0.675 THz frequency-modulated continuous-wave (FMCW) imagers developed by JPL(Jet Propulsion Laboratory) [7, 8, 27] and PNNL(Pacific Northwest National Laboratory) [28-30], both working in the real aperture focusing scheme, employing a main reflector to realize beam focusing and a sub-reflector to realize beam scanning. Taking advantages of the ranging capability, weaker signatures beneath the clothes is possible to be revealed in the active system [30]. For the aim of full-body coverage

at video rates, JPL group also developed multi-channel transceivers for their active system and realize 3D imaging with frame rate of 4 Hz [31, 32]. For active system, imaging based on the synthetic aperture scheme may have unique advantages over the real aperture scheme and has attracted growing attention recently. Different from the real aperture imaging, the fixed focal plane can be avoided due to the adaptive focusing algorithm, and objects can principally be imaged with equal resolution over a considerable range of depth in theory. Additionally, more versatile imaging schemes can be implemented for different kinds of applications. Recently, THz imaging with synthetic aperture focusing has attracted growing attention [11, 33, 34]. In 2013, a typical ISAR radar system is developed in 0.3 THz band by Fraunhofer Institute for High Frequency Physics and Radar Techniques [11]. Thanks to their advanced MMIC LNA technologies, the detection range of the system can reach far than 100 meters to obtain two-dimensional images.

In China, driving by Pioneers in Terahertz domain, such as Professor ShengGang Liu from University of Electronic Science and Technology of China, the THz technologies from sources, detectors to application systems are developing rapidly in recent years. Several Institutes and Universities have made efforts on Terahertz imaging for security and have developed Proof-of-State systems. For example, Capital Normal University, No.50 and No.38 Research Institutes of China Electronics Technology Group Corporation have done research on passive imaging in 0.3 THz and 0.1 THz band. University of Electronic Science and Technology of China has done research on ISAR imaging in 0.3 THz band. Institute of Electronics from Chinese Academy of Sciences, and University of Shanghai for Science and Technology have done research on THz active imaging in 0.3 THz and 0.1 THz band.

Nowadays, the imaging technology in THz band for security is progressing in a trend from the personal screen in near distance, to stand off imaging with far distance. Various new technologies are necessary to be developed to improve the performance of the system. Imaging with high frame rate for large field of view and synthesized aperture scheme may become more and more important in THz regime.

3. Image reconstruction algorithm

3.1 Image reconstruction of targets illuminated by terahertz gaussian beam based on synthetic aperture concept

In THz range, quasi-optics are universally used to achieve controlled propagation of radiation in free space. Employing Gaussian beams which are moderately well collimated with limited lateral extent transverse to their axis of propagation is the fundamental theory of quasi-optical techniques [35, 36]. Gaussian beam generation and Gaussian optical designs have come to play

an important role in the system design at THz wavelengths. To extending the synthetic aperture scheme to THz band, it's reasonable to start with the imaging reconstruction of targets under the illumination of THz Gaussian beam [37, 38].

Fig.3 gives a fundamental imaging scheme composed of the THz transceiver and the quasi-optics. The echoed fields scattered from the target are collected by the pan scanning of the Quasi-optical transceiver over a two-dimensional aperture, which including both the amplitude and the phase information. The task of the refocusing algorithm is to reconstruct the high resolution images based on the synthesis of the echoed field over the whole scanning aperture.

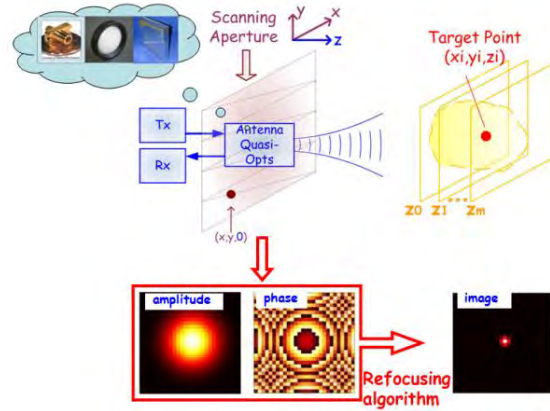


Fig. 3 THz imaging scheme based on Synthetic Aperture Concept

The THz transceiver of the imaging system are assumed to have center frequency ω_0 and bandwidth B , and launch a Gaussian beam propagating in the $+z$ direction with its phase center located at $(x, y, 0)$ and beam waist radius w_0 at the plane $z=0$. The transmitted field at the point (x', y', z') takes the form

$$A(x', y', z') = \frac{w_0}{w(z')} \exp\left[j \tan^{-1} \frac{2z'}{kw_0^2} - jkz'\right] \cdot \exp\left[-\frac{j2kz' + (kw_0)^2}{4z'^2 + (kw_0^2)^2} \rho^2(x', y')\right] \quad (1)$$

where $\rho(x', y') = \sqrt{(x'-x)^2 + (y'-y)^2}$ is the relative polar radius, and $w(z') = w_0 \sqrt{1 + (2z'/kw_0^2)^2}$ is the beam radius at the plane $z = z'$.

Considering a point target with unit “scattering coefficient” located at (x_i, y_i, z_i) , the echoed field $U(x, y, 0, \omega)$ can be measured after the THz transceiver is scanned in the plane $z=0$. Due to the roundtrip of the wave, the echoed field takes the form

$$U(x, y, 0, \omega) = A^2(x_i, y_i, z_i) = \left[\frac{w_0}{w(z_i)}\right]^2 \exp(-j2kz_i) \cdot \exp\left[-\frac{j4kz_i + 2(kw_0)^2}{4z_i^2 + (kw_0^2)^2} \rho^2(x_i, y_i)\right] \quad (2)$$

Based on the theory of phase shift migration, the echoed wave at an arbitrary point (x, y, z) from the target illuminated by a source located at the same point (x, y, z) take following expression in

time domain as

$$u(x, y, z, t) = \iiint FT_{2D}[U(x, y, 0, \omega)] \cdot \exp[j(k_x x + k_y y + k_z z + \omega t)] dk_x dk_y d\omega \quad (3)$$

According to the exploding source model [39], the reconstructed image is then taken to be the echoed field at time $t = 0$.

Based on Eqs.(2) and (3), the 3D reconstructed point-spread function (PSF) of the point target under the illumination of Gaussian beam defined in Eq.(1) can be derived based on the phase shift migration algorithm with following expression

$$|u(x, y, z)| = 2\pi B \frac{w_0^2}{w(z_i)w(z-z_i)} \exp\left\{-\frac{2[k_0 w_0 \rho(x_i, y_i)]^2}{(k_0 w_0^2)^2 + 4(z-z_i)^2}\right\} \cdot \text{sinc}\left[\frac{2B}{c_0}(z-z_i)\left\{1 + 2\rho^2(x_i, y_i) \frac{4(z-z_i)^2 - (k_0 w_0^2)^2}{[(k_0 w_0^2)^2 + 4(z-z_i)^2]}\right\}\right] \quad (4)$$

By employing the 3 dB power decreasing criterion, the range resolution in the z-direction and the cross range resolutions in x- and y-directions can be evaluated based on Eq. (4). Along the axis $\rho = 0$, Eq. (4) is simplified to

$$|u(x, y, z, 0)| = 2\pi B \frac{w_0^2}{w(z_i)w(z-z_i)} \text{sinc}\left[\frac{2B}{c_0}(z-z_i)\right] \quad (5)$$

The corresponding range resolution in the z-direction is

$$\delta_z \approx 0.44 \frac{c_0}{B} \quad (6)$$

In the plane $z = z_i$, Eq. (4) is simplified to

$$|u(x, y, z, 0)| = 2\pi B \frac{w_0}{w(z_i)} \exp\left(-\frac{2\rho^2(x_i, y_i)}{w_0^2}\right) \quad (7)$$

The cross range resolutions in x- and y-directions are

$$\delta_x = \delta_y \approx 0.83w_0 \quad (8)$$

Additionally, the up limit of the spatial sampling intervals in x and y directions to avoid aliasing are derived based on the spectrum analysis in wave number domain as following:

$$\Delta x = \Delta y \approx \frac{\pi w_0}{4.29} \quad (9)$$

Fig.4 shows the comparison of the simulation and theoretical results of the reconstructed images for a point target located at $(0, 0, 500 \text{ mm})$ imaged by a 0.2 THz transceiver with bandwidth 15 GHz and beam waist radius 2.7 mm .

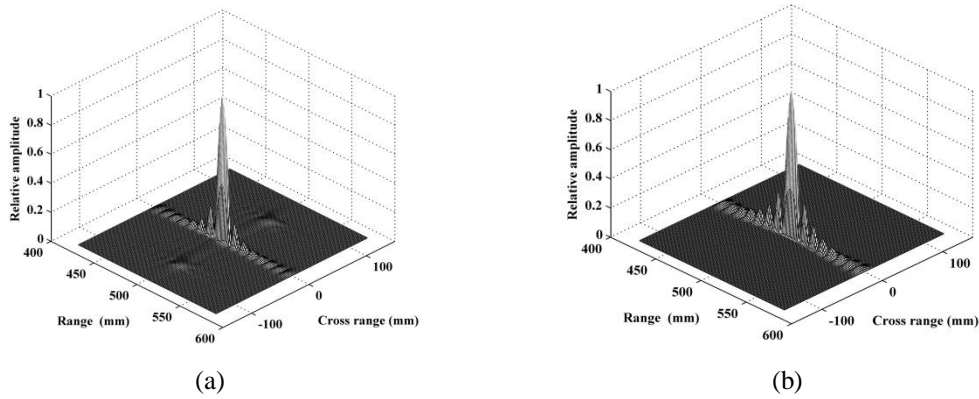


Fig. 4 Reconstructed PSF in $x(y)$ - z plane. (a) simulation, (b)theory

To perform proof-of-principle experiments, a prototype imager with quasi-optics transceiver is developed in 0.2 THz band. The Gaussian beam waist radius of the gaussian beam launched by the transceiver is measured to be 2.7 mm . A target with many metal strips spaced from 1 mm to 6 mm in the left part and from 1 mm to 8 mm in the right part is imaged as shown in Fig. 5(a). Fig. 5(b) illustrates the well focused wide-band reconstructed image on dB scale which shows the cross range resolution is about 2 mm . This result agrees well with the theoretical value calculated based on Eq.(8).

To study the sampling interval requirement, a plastic gun was imaged by the sampling changing from 1 mm to 3 mm in the cross range. It's found from Fig.6 that, when the sampling intervals is equal or less than the theoretical requirement 1.94 mm (based on Eq.(9)), the changing of the sampling does not affect the image quality. When the sample goes up to 3 mm , the obvious aliasing can be observed from the reconstructed image.

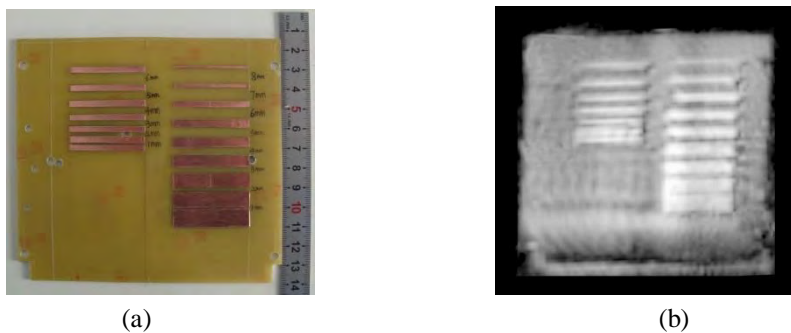


Fig. 5 (a) Optical image (b) 0.2THz image of metal strips

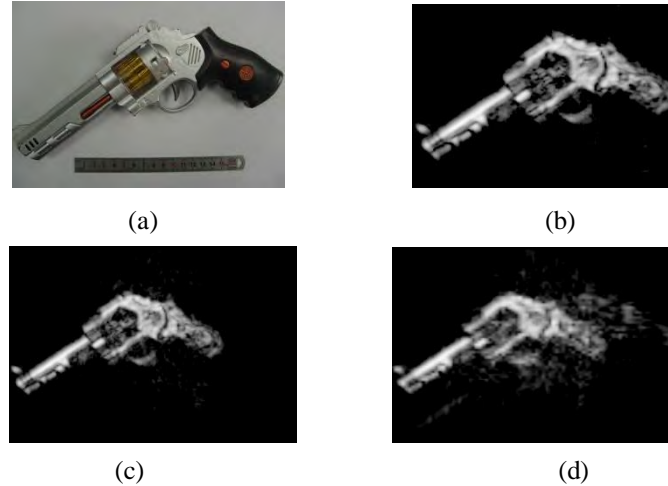


Fig. 6 (a) Optical image and (b),(c),(d) 3-D THz image of a plastic cap gun with 1 mm, 2 mm, 3 mm spatial sampling intervals.

3.2 THz image reconstruction based on sparse information

The methods to reconstruct image with sparse information may greatly reduce the complexity and the cost of a THz imaging system. In conventional single frequency imaging, only 2D images can be reconstructed with a fixed restoration range distance z_0 . For an ideal point target located at (x_i, y_i, z_i) with an “scattering coefficient” σ_i , the reconstructed 2-D point spread function (PSF) can be derived as [40]

$$|\tilde{s}_i(x, y)| = \sigma_i \frac{w_0^2}{w(z_i)w(z_i - z_0)} \cdot \exp\left\{-\frac{2\rho^2(x_i, y_i)}{[w(z_i - z_0)]^2}\right\} \quad (10)$$

Here $w(z_i - z_0)$ is the diffused waist radius of the transmitting beam at the plane $z_i - z_0$. This means the image defocus in a way like the diffusion of the Gaussian beam [40]. When restoration range distance z_0 is exactly equal to target distance z_i , the best focused image can be obtained. It's seen that, the image will become defocused as the restoration distance z_0 differ from the target distance z_i . This means targets with different range distance z_i cannot be focused in single frequency imaging simultaneously. To solve this problem, the concept of entropy was borrowed here to evaluate the quality of the 2D THz image. Fig.7 shows the resolution and the entropy for the image of a point target located at (x_i, y_i, z_i) with different restoration distance z_0 . It's seen that when $z_0 = z_i$, the best resolution and the minimum entropy of the image achieved at the same time. And the better focusing is equivalent to the smaller image entropy. Based on such concept, an adaptive focusing algorithm [40] with the combination of minimum entropy theory and the stage by stage approaching (SSA) method [41] was developed to improve the Depth of Focus in single frequency image reconstruction.

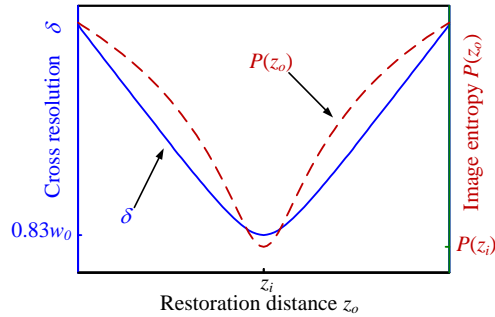


Fig. 7 Cross resolution and Image entropy of THz image

Fig.8 shows the 0.2 THz experimental results on three metal objects, which are located at 0.33 m, 0.53 m and 0.83 m, respectively, with maximum range depth about 0.5 m. Firstly, images are reconstructed based on conventional holography with different restoration distances $z_0=0.33\text{ m}$, 0.53 m and 0.83 m. Fig.8(b), (c) and (d) show the images which are only focused individually on knife, pliers and pistol. Fig.8(e) shows the reconstructed image based on the proposed adaptive focusing algorithm. It's seen that all the three targets can be focused which verify the effectiveness of the proposed adaptive focusing method.

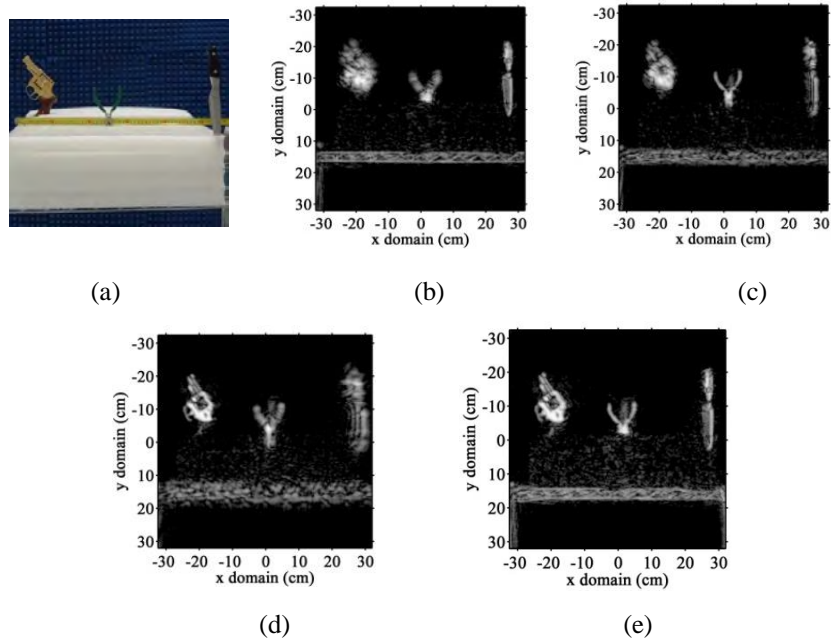


Fig. 8 (a), (b) and (c) are THz images reconstructed based on conventional holography with restoration distance 0.33 m, 0.53 m and 0.83 m, respectively. (d) optical image of the target. (e) THz image by ME-AF algorithm.

Another concept of 3D imaging with sparse information is to reconstruct image of 3D surface layer with sparse random step frequencies [42]. The method including two steps: Firstly, the echoed data gathered on random step frequency with reduced frequency numbers is applied to evaluate the range profile of the 3D surface layer. Then, a de-ambiguity procedure is proposed to

compress the maximum non-ambiguous range and recover the complete information for 3D image reconstruction. A proof-of-state experiment was conducted in 0.2 THz band with signal bandwidth 19.2 GHz . Three targets in Fig.9 (a) are located in different distances with maximum range of 0.7 m . In the experiments, only 20 frequency points which are much less than the anti-aliasing requirement for conventional range reconstruction are used. Fig.9(b) and (c) show the cross range image and the range profile based on 20 random frequencies and the proposed algorithm in [42]. Fig.9.(d) and (e) show the corresponding results with 20 uniformly sampled frequencies and the conventional reconstruction method. It's seen that, the proposed method is effective to accurately recover the targets based on sparse information. Compared to the single frequency reconstruction based on minimum entropy theory, the complex iteration process can be avoided in the sparse random frequencies approach, and hence result in a more efficient reconstruction, but at the cost of multi-frequencies.

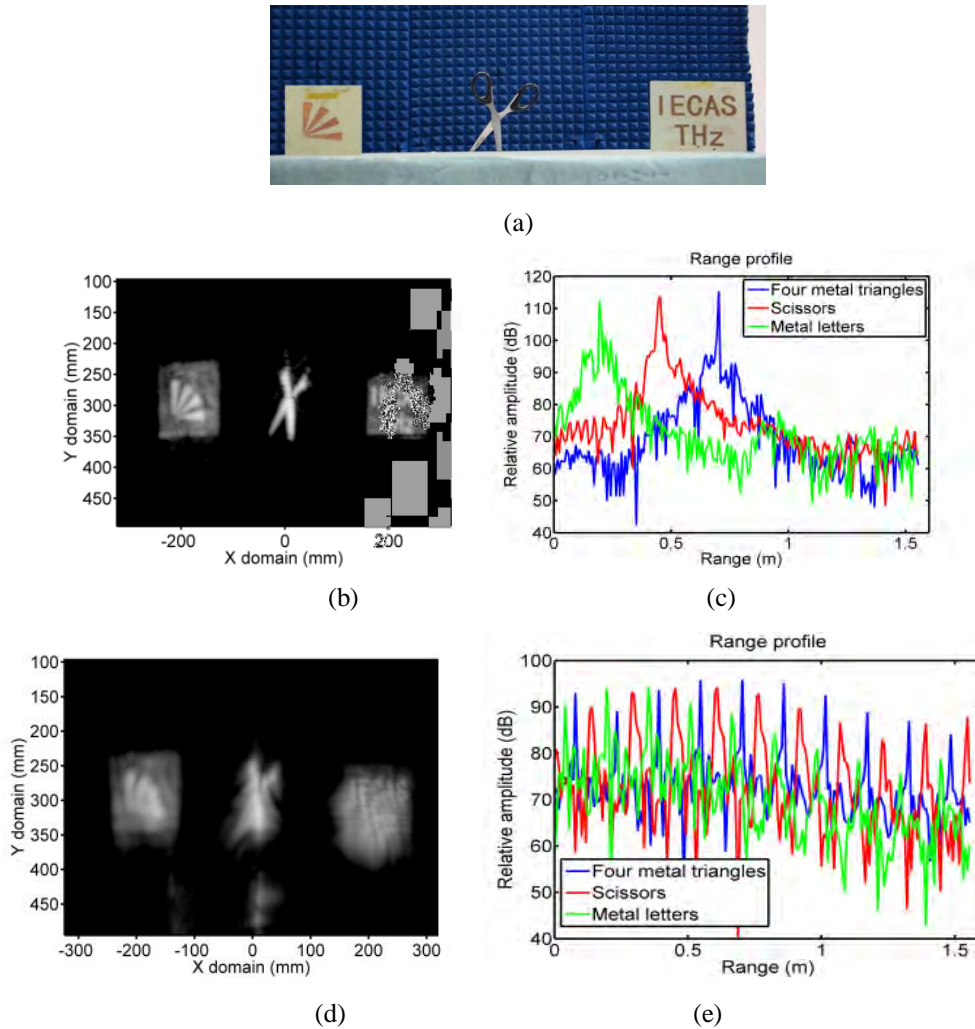


Fig. 9 (a) Optical image of the targets, (b) cross range image and (c) range profile based on method in [42] with 20 random frequencies, (d) cross range image and (e) range profile based on conventional reconstruction with 20 uniform frequencies.

4. Terahertz 3D imaging with synthesized aperture technology

In this section, the synthetic aperture technique was extended for terahertz 3D imaging system with fan-beam scanning and real-time capability. The basic imaging scheme was shown in Fig.10. The system employs a pillbox-like transceiver antenna to generate a fan-beam [43]. The beam in the y - z plane is well focused at the distance d from the antenna aperture by a concave main-reflector. In the x - z plane, the wave diffuses from the antenna aperture to form wide side of the fan-beam in the x direction. Based on the quick rotation of the small sub-reflector, the fan-beam can quickly scan along the y -direction. With the combination of line scan along the x -direction by the motorized stage, the phase and amplitude of echoed signal can be collected over a large 2-D aperture to reconstruct a focused image of target. For the above imaging scheme, high resolution in the y -direction can be directly achieved based on focusing of the main reflector, and high resolution in the x -direction can be obtained by aperture synthesized technique. In z direction, frequency modulation continuous wave (FMCW) was transmitted to achieve range resolution.

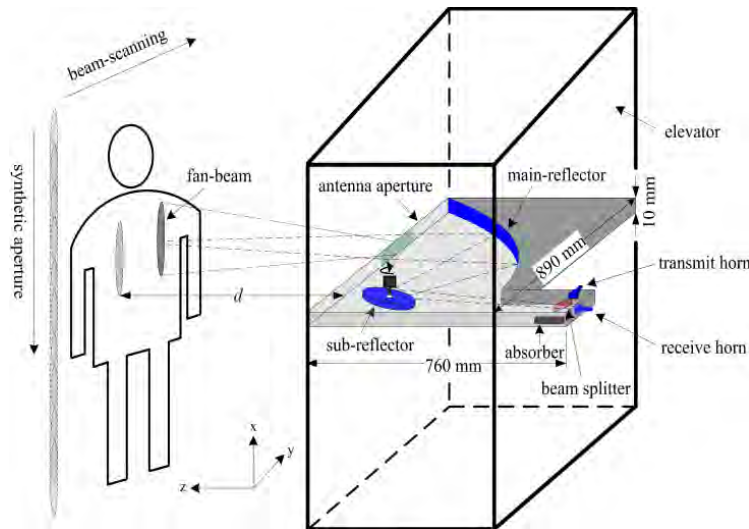


Fig. 10 THz imaging scheme based on the combination of fan-beam scanning and aperture synthesized techniques.

Fig. 11 shows the basic imaging geometry. Assuming the radiation aperture of the fan-beam antenna is in the plane $z=d$, and a general target is assumed to have a reflectivity distribution function $f(x', y', z')$. The acquired scattering parameter S_{21} by frequency sweeping measurement is sampled over 2-D scanned aperture and labeled as $s(x, y, k)$ in the following, where c is the light velocity, ω is the temporal angular frequency, and $k = \omega/c$ is the wave-number. Then the 3D image of targets can be derived based on the reconstruction algorithm as

$$f(x', y', z') = \text{FT}_{2\text{D}(k_x, k_z)}^{-1} [\text{FT}_{1\text{D}(x)} [s(x, y', k)] e^{-jk_z d}] \quad (11)$$

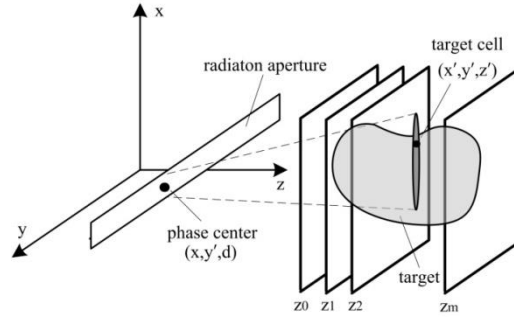


Fig. 11 Geometry for the theoretical analysis.

From Eq.(11), we can find that the 3-D image reconstruction is just a quasi 2-D problem. This is a very important advantage of the proposed fan-beam scanning imager which makes the data easy to process. In practical imaging processing, the data are discretely sampled with uniform intervals in the space and frequency domain. Hence, the 2-D inverse FFT in Eq.(11) will not be directly used because the sampling data are non-uniformly sampled in the k_z domain. Interpolation techniques are necessary to be employed to real-time data processing for the 3-D algorithm.

A prototype setup has been developed based on the THz Vector Network Analyzer and the fan-beam scanning antenna in 2012, for the demonstration of basic imaging scheme and reconstruction algorithm [44]. To realize 3D real-time imaging with high quality, a series of key components were latterly developed, optimized and integrated.

To satisfy the requirement of real-time capability, the FMCW transmitter with broad bandwidth and high frequency modulation rate is necessary. In our system design, the modulation time of 10 microseconds with max bandwidth about 30 GHz was realized at the center frequency 0.3 THz has been accomplished based on the combination of quick digital modulation, analogical phase locking and THz frequency multiplying technologies. In the transmitter, the direct digital waveform synthesis (DDWS) and the phase locked loops are integrated to obtain the FMCW signal in Ku band, and then driving the THz multiplication chain to obtain the required signal in sub-THz band, as shown in Fig.12. The frequency nonlinearity problem, which is mainly introduced by the THz multiplication with high order, may heavily degrade the imaging quality. Thanks to the DDWS technique employed in the transmitter, the phase error resulted from the frequency modulation nonlinearity can be pre-compensated in the baseband of the transmitter and then greatly improve the imaging quality.

Here given a typical experimental result on the frequency nonlinearity pre-compensation, the return wave is obtained from the reflection of a metal plane. Fig.13 gives the range profiles before and after pre-compensation. It's seen that the image quality can be greatly improved with the compensation of the frequency nonlinearity.

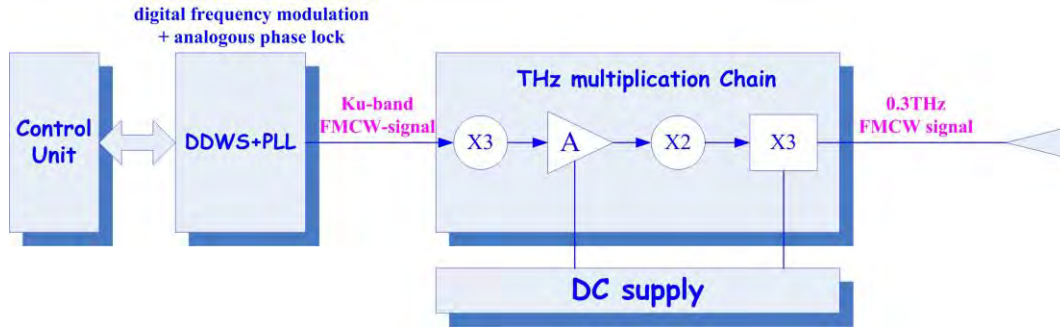


Fig. 12 Scheme for 0.3 THz FMCW transmitter.

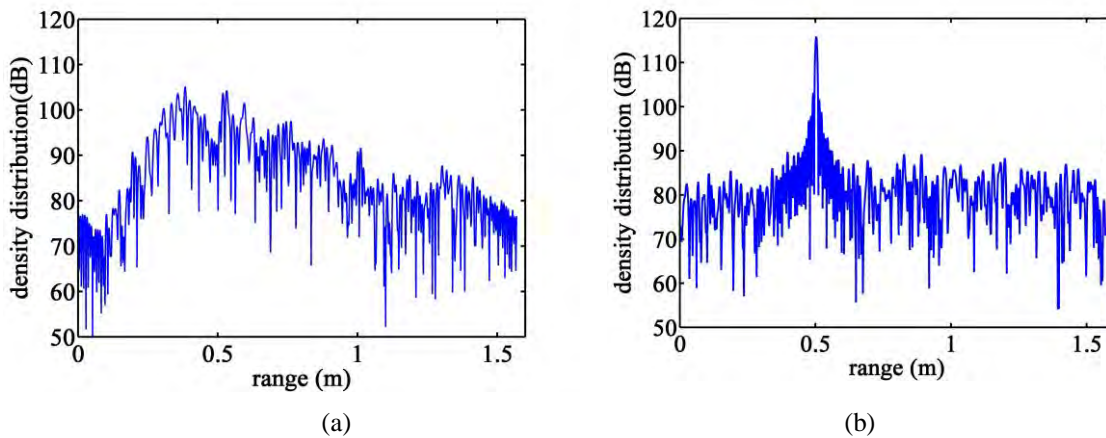


Fig. 13 Range profile (a) before pre-distortion compensation, (b) after pre-distortion compensation.

The function of the receiver is to obtain the amplitude and the phase of the return wave for image reconstruction. To effectively receive the wideband signal, the heterodyne scheme with de-chirp and IQ demodulation in intermediate frequency band was employed.

To further improve the beam-scanning efficiency and the beam-pattern, the original antenna structure used in [44] was latterly optimized on two aspects (as illustrated in Fig.14). Firstly, the sub-reflector was designed to a more symmetrical structure. Hence, one time of rotation from the sub-reflector can provide several times of beam-scanning in y direction which results in a better efficiency. Secondly, the main reflector was chosen as shaped concave instead of original elliptical reflector. Based on the combination of the approach developed in [43], the antenna working at 0.3 THz was designed, optimized and fabricated. Fig.15 shows the measured patterns for three different scanning positions.

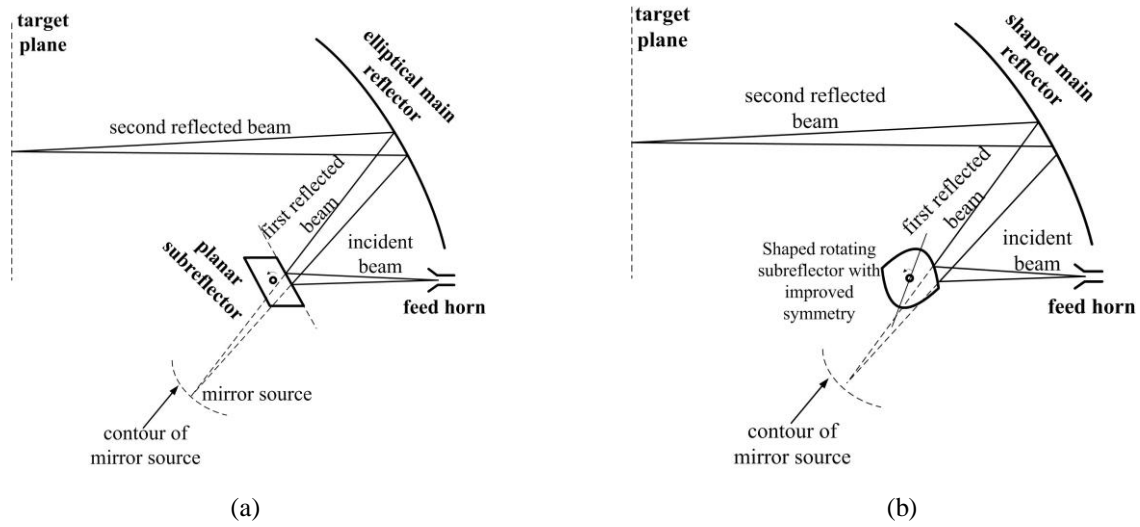


Fig. 14 (a) original antenna topology used in [44] (b) optimized antenna topology

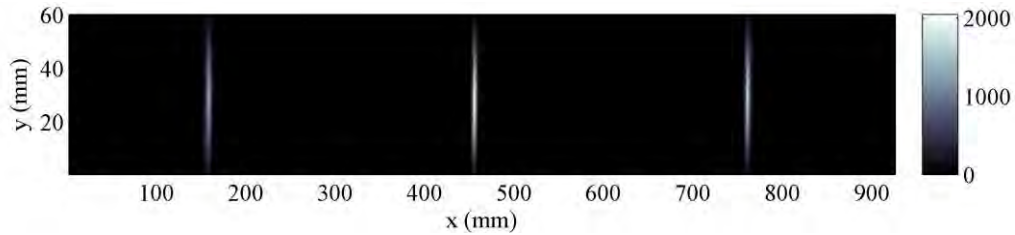


Fig. 15 Measured beam scanning pattern for subreflector located in three different angle.

Based on the transceiver and the optimized fan-beam scanning antenna, the 3D imaging system in 0.3 THz band was integrated. In the imaging reconstruction, the gathered 3D return wave data matrix was divided into 16 parts, and then the algorithm was performed based on the multi-core parallel processing with advanced DSP techniques, to satisfy the real-time capability. The total time for obtain a 3D image (including the scanning and the reconstruction) for a field of view 60 cm×180 cm is about 3 seconds. The cross range resolution is 5 mm×5 mm, and the range resolution is 8 mm. Fig. 16 shows the 0.3 THz images of a mannequin with a concealed metal gun. Based on the obtained 3-D image data on one time of scanning, we can observe the target from different directions. Fig. 16(b) is a typical front view. Fig. 16(a) and (c) give the 30 degree left and right side view, respectively. It's seen that the concealed gun can be clearly recognized in these images.

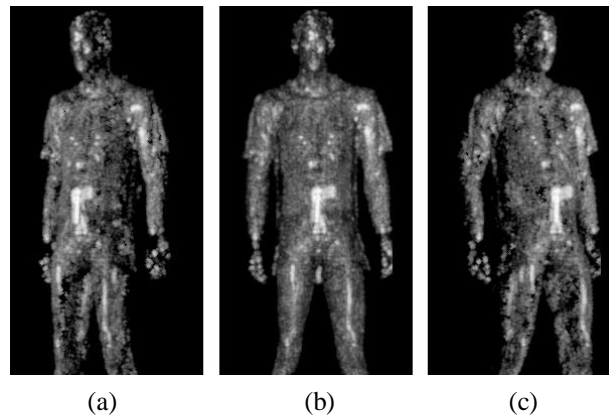


Fig. 16 THz 3D images of a mannequin with a concealed metal gun. (a) 30 degree left side view, (b) front view, (c) 30 degree right side view.

5. Conclusion

In this paper, some background on THz imaging for security were discussed, and the recent progress on the research of THz imaging and sensing at IECAS was summarized both in theoretical and some system engineering aspects. To extend the synthesized aperture concept to THz band, the relationships between the image qualities and the parameters of quasi-optical transceivers were quantitatively evaluated for the guidance of system development. Concepts on THz image reconstruction with sparse information were also introduced to reduce the complexity of systems. Based on the combination of the synthesized aperture concept, fan-beam scanning antenna, and THz FMCW transceiver, 3D imaging system in 0.3 THz band with real-time capability was developed, which has potential applications for security screen.

References

- [1] D. M. Mattleman, M. Gupta, and R. Neelamani. "Recent advances in terahertz imaging". *Applied Physics B.*, 68:1085-1094(1999).
- [2] D. Dragoman, M. Dragoman, Terahertz fields, et al.. *Progress in Quantum Electronics*, 28(1): 1-66(2004).
- [3] Z. Popović, and E. N. Grossman. "THz Metrology and Instrumentation". *IEEE Trans. Terahertz Science and Technology*, 1(1): 133-144(2011).
- [4] Carter M. Armstrong. "The truth about Terahertz". *IEEE Spectrum*, 36-41(2012).
- [5] XiaoXia Yin, Brian W.- H. Ng, Derrek Abbott. "Terahertz Imaging for Biomedical Applications". Springer, (2012).
- [6] R. Appleby, H. B. wallace. "Standoff detection of weapons and contraband in the 100 GHz to 1 THz region". *IEEE Trans. Antennas Propagat.*, 55, 11, 2944-2956 (2007).

- [7] K. B. Cooper, R. J. Dengler, N. Llombart, et al.. "Penetrating 3-D imaging at 4- and 25-m range using a submillimeter-wave radar". *IEEE Trans. Antennas Propagat.*, 56, 12, 2771-2778 (2008).
- [8] K. B. Cooper, R. J. Dengler, Nuria N. Llombart, et al.. "THz imaging radar for standoff personnel screening". *IEEE Trans. Terahertz and Technology*, 1, 1, 169-182 (2011).
- [9] Q. Song, Y. J. Zhao, A. Redo-Sanchez, et al.. "Fast continuous terahertz wave imaging system for security". *Optics Communicatios*, 282, 2019-2022 (2009).
- [10] E. Grossman, C. Dietlein, J. Ala-Laurinaho, et. al. "Passive terahertz camera for standoff security screening". *Applied Optics*, 49, 19, 106-120 (2010).
- [11] S. Stanko, M. Caris, A. Wahlen, et. al.. "Millimeter Resolution with Radar at Low Terahertz". in Radar Symposium (IRS), Dresden, Germany, 19-21 (2013).
- [12] D. Zimdars, J. S. White, G. Stuk, et al.. "Large area terahertz imaging and non-destructive evaluation applications". in *Proc. 4th International Workshop on Ultrasonic and Advanced Methods for Nondestructive Testing and Material Characterization, UMass Dartmouth, N. Dartmouth, MA*, 63-66(2006).
- [13] J. B. Jackson, J. Bowen, G. Walker, et al. "A survey of terahertz applications in cultural heritage conservation science". *IEEE Trans. Terahertz and Technology*, 1, 1, 220-231 (2011).
- [14] Joo-Hiuk Son. "Terahertz electromagnetic interactions with biological matter and their applications". *Journal of Applied Physics*, 105: 102033 (2009).
- [15] Z. D. Taylor, R. S. Singh, D. B. Bennett, et. al.. "THz Medical Imaging: in vivo Hydration Sensing". *IEEE T. Terahertz Science and Technology*, 1, 1, 201-219 (2011).
- [16] Bessou M, Duday H, Caumes J P, et al.. "Advantage of terahertz radiation versus X-ray to detect hidden organic materials in sealed vessels[J]". *Optics Communications*, 285(21-22):4175-4179 (2012).
- [17] M.J. Rosker, H.B. Wallace. "Imaging through the atmosphere at terahertz frequencies". in *Proceedings of IEEE/MTT-S International Microwave, Symposium*, 773-776 (2007).
- [18] Gatesman, A. J., Danylov, A., Geyette, et. al.. "Terahertz Behavior of Optical Components and Common Materials". *Proceedings of SPIE*, 6212, 62120E -6210E-12 (2006).
- [19] Dickinson, J.C., Goyette, T. M., Gatesman, A.J., Joseph, et. al.. "Terahertz imaging of subjects with concealed weapons". *Proceedings of SPIE*, 6212, 6210Q1-1-6210Q1-12 (2006).
- [20] Bjarnson, J.E. Chan, T. L. J., Lee, A. W. M, Celis M. A., et. al.. "Millimeter-wave, terahertz and mid-infrared transmission through common clothing". *Appl. Phys. Lett.* 85, 4, 519-521 (2004).
- [21] R. Appleby, and R. N. Anderton. "Imaging and Sensing from 100GHz to 1THz". *Loughborough Antennas & Propagation Conference*, 84-88 (2009).
- [22] "IEEE Standard for Safety Levels with Respect to Human Exposure to Radio Frequency Electromagnetic Fields, 3kHz to 300 GHz". IEEE Std C95.1TM-2005, IEEE 3 Park Avenue, New York, NY 10016-5997, USA.
- [23] Chris Mann, Milton Park, "First demonstration of a vehicle mounted 250GHz real time passive imager". *Proc. of SPIE*, 7311:73110Q-1 (2009).
- [24] C. Mann. "Real Time Passive Imaging at 250 GHz for Security: Technology and Phenomenology". International Conference on Electromagnetics in Advanced Applications, 2009:1013-1015 (2009).
- [25] T. May, G. Zieger, S. Anders, et. al.. "Safevisitor: visible, infrared, and terahertz object recognition for security screening application". *SPIE* 7309, 73090E (2009).
- [26] E. Heinz, D. Born, G. Zieger, et. al.. "Progress report on Safe VISITOR approaching a practical instrument for terahertz security screening". *SPIE* 7670, 767005 (2010).

- [27] K. B. Cooper, R. J. Dengler, N. Lombart, et.al.. "Fast high-resolution terahertz radar imaging at 25 meters". *SPIE* 7671, 76710Y (2010).
- [28] David M. Sheen, Douglas L. McMakin, Jeffrey Barber b, et.al.. "Active imaging at 350 GHz for security applications". *Proc. of SPIE*, 6948:69480M (2008).
- [29] D.M. Sheen, T.E. Hall, and R. H. Severtsen, et.al., "Active wideband 350GHz imaging system for concealed-weapon detection," *Proc. of SPIE*, 2009, 7309:73090I.
- [30] David M. Sheen, Douglas L. McMakin, Thomas E. Hall, et.al.. "Active millimeter-wave standoff and portal imaging techniques for personnel screening". *IEEE Conference on Technologies for Homeland Security*, 440-447 (2009).
- [31] T. A. Reck, J. Siles, C. Jung, et al., "Array Technology for Terahertz Imaging". *Proc. SPIE*, 8362: 836202 (2012).
- [32] K. B. Cooper, T. A. Reck, C.Jung, et al.. "Transceiver Array Development for Submillimeter-Wave Imaging Radars". *Proc. SPIE*, 8715:87150A (2013).
- [33] V. Krozer, T. Löffler, J. Dall, et. al, "Terahertz imaging systems with aperture synthesis techniques". *IEEE Trans. Microw. Theory Tech.*, 58, 7, 2027-2039 (2010).
- [34] F. Friederich, W. V. Spiegel, M. Bauer, et. al.. "THz Active imaging systems with Real-time Capabilities". *IEEE Transactions on Terahertz Science and Technology*, 1, 1, 183-200 (2011).
- [35] P. F. Goldsmith. "Quasi-optical techniques". *Proc. Of the IEEE*, 80, 11, 1729-1747 (1992).
- [36] P. Goldsmith. *Quasioptical Systems: Gaussian Beam Quasioptical Propagation and Applications*. IEEE(1998).
- [37] Shengming Gu, Chao Li, Xiang Gao, et al.. "Three-dimensional image reconstruction of targets under the illumination of terahertz Gaussian beam-theory and experiment [J]". *IEEE Transactions on Geoscience and Remote Sensing*. 51(4): 2241-2249 (2013).
- [38] Zhaoyang Sun, Chao Li, Shengming Gu, et al.. "Fast Three-Dimensional Image Reconstruction of Targets Under the Illumination of Terahertz Gaussian Beams with Enhanced Phase-Shift Migration to Improve Computation Efficiency". *IEEE Trans. On Terahertz Science and Technology*, 4 (4), 479-489 (2014).
- [39] D. Loewenthal, L. Lu, R. Roberson, and J. Sherwood. "The wave equation applied to migration". *Geophys. Prospect.*, 24, 2, 380-399 (1976).
- [40] Zhaoyang Sun, Chao Li, Xiang Gao, et al.. "Minimum-Entropy Based Adaptive Focusing Algorithm for Image Reconstruction of Terahertz Single Frequency Holography with Improved Depth of Focus". *IEEE Trans. On Geoscience and Remote Sensing*, 53, 1, 519-526 (2015).
- [41] X. Li, L.Guosui, and N. Jinlin. "Autofocusing of ISAR images based on entropy minimization". *IEEE Trans. Aerosp Electron. Syst.*, 35, 4, 1240-1252, (1999).
- [42] Wei Liu, Chao Li, Zhaoyang Sun, et.al.. "Three-dimensional sparse image reconstruction for terahertz surface layer holography with random step frequency". *Optics Letters*, 40, 14, 3384-3387 (2015).
- [43] Xiang Gao, Chao Li, Shengming Gu, et al.. "Design, Analysis and Measurement of a Millimeter Wave Antenna Suitable for Stand off Imaging at Checkpoints". *Journal of Infrared, Millimeter, and Terahertz Waves*, 32, 9, 1-14 (2011).
- [44] Shengming Gu, Chao Li, Xiang Gao, et al.. "Study of Terahertz Aperture Synthesized Imaging with Fan-Beam Scanning for Personnel Screening". *IEEE Transactions on Microwave Theory and Technology*, 60, 12, 3877-3885 (2012).